Rise velocity verification of bubble-floc agglomerates using population balance in the DAF process

Dong-Heui Kwak, Heung-Joe Jung, Sun-Beum Kwon, Eun-Ju Lee, Chan-Hee Won, Jae-Wook Lee and Seung-Joon Yoo

ABSTRACT

The dimension of the separation zone in the dissolved air flotation (DAF) process is practically determined by the rise velocity of the bubble-floc agglomerates: flocs attached to several bubbles. To improve the flotation velocity and particle removal efficiency in the DAF process, many researchers have tried to attach as many bubbles as possible to flocs. In this study, the rise velocity of bubble-floc agglomerates, considered to be the most important factor in designing the separation zone of the flotation tank in the DAF process, was investigated on the basis of comparison between theoretical and observed results. The observed rise velocity measured by a particle image analyser (PIA) and the predicted value, however, did not show similarity, in contrast to what we had expected. Furthermore, the simulated results using population balance to predict the maximum number of attached bubbles on a floc were too impractical to accept under the practical condition of the surface of the floc if there was no change of bubble size. These findings led us to suggest that there were three possible causes which could conceivably explain the observations. It was suggested that the differences between predicted and observed values could be attributed to one or more of the possible causes.

Key words | agglomerate, bubble, dissolved air flotation, floc, population balance, rise velocity

Dong-Heui Kwak
Seung-Joon Yoo (corresponding author)
Division of Environmental and Chemical Engineering,
Seonam University, 720, Kwangch-dong,
Namwon, Jeonbuk 590-711,
Korea
Tel.: +82-63-620-0230
Fax: +82-63-620-0211
E-mail: *sjyoo001@hanmail.net*

Heung-Joe Jung
Department of Biological Engineering,
Singyung University,
1485, Namyang-dong, Hwaseong,
Kyungki-do 445-852, Korea

Sun-Beum Kwon
Water Research Center,
Korea Institute of Water and Environment,
Korea Water Resources Corporation,
462-1, Jeonmin-dong,
Yusung-gu, Daejeon 305-730, Korea

Eun-Ju Lee
Department of Civil and Environmental Engineering,
Kongju National University,
182, SinKwan-dong, Kongju,
Chungnam 314-701, Korea

Chan-Hee Won
Department of Environmental Engineering,
Chonbuk National University,
664-14, 1Ga Deokjin-dong, Jeonju-city,
Jeonbuk 561-756, Korea

Jae-Wook Lee
Department of Chemical and Biochemical Engineering,
Chosun University, 375, SeoSeok-dong,
Dong-gu, Kwangju 501-759, Korea

INTRODUCTION

The main advantage of dissolved air flotation (DAF) in the water treatment process is its small dimensions, which can be achieved by the short solid-liquid separation time, compared with conventional gravity sedimentation. The dimension of the separation zone in the DAF process is practically determined by the rise velocity of the bubble-floc agglomerates, which are flocs attached by several bubbles. Several models have described not only the collision between bubbles and particles but also the attendant kinetics such as the rise velocity of bubble-floc agglomerates

doi: 10.2166/aqua.2009.021

in the DAF process applied to water treatment plants (Malley & Edzwald 1991; Schers & Van Dijk 1992; Fukushi *et al.* 1995; Jung *et al.* 2006).

In the field of DAF processes, over the past few years, the hydraulic loading rates, which are directly related to the treatment capacity, have increased as follows: from 2–3 m h^{-1} (or less than 5 m h^{-1}) in the 1920s to 20–25 m h^{-1} in 1996 and to the current 40 m h^{-1} (Haarhoff & Edzwald 2004). For the determination of the depth in designing the separation zone of the DAF process, there is the limit that the smallest bubble group of the bubble cloud layer or the lowest level of bubble-floc agglomerates should not be carried over to the next process. It is not only the bubble properties but also the flow structure which could be important for carry-over problems. When only the size limit is considered, in removing bubble-floc agglomerates effectively in the separation zone, the larger bubble size will be desirable because it makes the rise velocity higher than the smaller bubble. Since the large bubbles, however, give rise to a low collision efficiency between bubbles and flocs, the smaller bubble is basically applied to the water treatment process. Moreover, the bubble size is hard to control flexibly in the field. Therefore, the practical rise velocity of bubble-floc agglomerates is determined by the number or the size of bubbles attached to a floc if there is no control of bubbles artificially (Kwak *et al.* 2002).

On the other hand, many of the DAF models have considered the complex processes and interactions between bubbles and flocs. Schers & Dijk (1992) proposed the flotation velocity of bubble-floc agglomerates and the flotation velocity model equation of bubble-floc agglomerates. The velocity of the agglomerate calculated through the bubble-floc volume ratio by inducing the Stokes equation was applied when it is less than Reynolds No. 1. The maximum volume fraction of air in bubble-floc agglomerates, β, is 0.8 because it is physically impossible to accumulate bubbles in layers in the case of a floc diameter of 200 μm and an average bubble diameter of 40 μm (Liers *et al.* 1996). It has been shown that the number of attached bubbles to a floc is in the order of 1 to 100, thus corresponding to β-values of 0.008–0.8 (Tambo & Fukushi 1985; Tambo *et al.* 1985). Fukushi *et al.* (1995) predicted the number of attached bubbles to a floc for the estimation of the initial collision-attachment factor and for the verification of the progress of bubble-floc attachment using population balance. The approach of population balance describes collisions between bubbles and particles and the fundamental behaviours of bubble-floc agglomerates through numerical kinetic expression of population. Leppinen *et al.* (2001) proposed a kinetic model that modified that of Fukushi *et al.* (1995) in order to predict the rise velocity of bubble/floc agglomerates during flotation. This rise velocity is dependent on a number of factors including the bubble size, the particle or floc size, the density of bubble and flocs, the viscosity of water, the number of bubbles attached on a floc and the residence time of fluid within the contact zone.

However, the estimation of the rising velocity of the bubbles or bubble-floc agglomerates from Stokes' law is much more complicated than that of single bubbles because the sizes of bubbles are not uniform. Few general equations are available for the prediction of the size distribution of bubbles from the rising velocities (Rodrigues & Rubio 2003). In addition, it is still difficult to measure the exact number of bubbles attached to a floc in the separation zone of a flotation tank.

In this study, the rise velocity of bubble-floc agglomerates was verified by comparison between the observed results and the predicted values, which is considered mainly as a design parameter of the separation zone in DAF processes. This paper first presents the results of the theoretical prediction to estimate the number of bubbles attached to a floc by the kinetic model using population balance, which has been improved gradually (Fukushi *et al.* 1995; Leppinen *et al.* 2001), for a given influent. Second, the predicted results are compared with the observed data calculated on the basis of the rise velocity of bubble/floc agglomerates. The prediction procedure using the model is implemented using the observed data, followed by checking to see whether the prediction can be used to calculate the number of bubbles attached to a floc and to estimate the parameters of the model by best-fit of the observed data. Finally, to verify the rise velocity of bubble-floc agglomerates, we considered the feasible causes of the difference in terms of the number and the size aspects of bubbles on a floc.

THEORETICAL APPROACH

The population balance for describing the process of bubble-floc collision and attachment was formulated by counting the number of flocs attached, i-bubbles n_i, at mixing time t. On the basis of the assumptions reported by Fukushi et al. (1995) and modified by Leppinen et al. (2001), the number of flocs attached, i-bubbles n_i, is represented by the ordinary differential equations as follows:

$$\frac{dn_0}{dt} = -k\alpha_0 n_0 n_{\text{bubbles}} \quad (1)$$

$$\frac{dn_i}{dt} = k\alpha_{i-1}n_{i-1}n_{\text{bubbles}} - k\alpha_i n_i n_{\text{bubbles}}, \quad i = 1 \text{ to } i_{\max} \quad (2)$$

where k is the turbulent collision rate constant represented by the following equation.

$$k = aG(d_p + d_b)^3 \quad (3)$$

where the coefficient a is 0.385 according to Tambo et al. (1981), whereas Suffman & Turner (1956) derive a as 0.209, and G is the velocity gradient ($1\,s^{-1}$). The number of bubbles per unit volume, n_{bubbles}, is described using the bubble volume concentration in the contact zone (ϕ) as:

$$n_{\text{bubbles}} = \frac{\phi}{\pi d_b^3/6} \quad (4)$$

Adhesion efficiency (α) is determined by the ratio of size between bubble and floc and the number of attached bubbles can be written as:

$$\alpha_i = \begin{cases} \alpha_0\left(1 - i\frac{d_b^2}{d_p^2}\right), & i = 1 \text{ to } i_{\max} - 1 \\ 0, & i = i_{\max} \end{cases} \quad (5)$$

With the substitution of Equations (3) to (5) into Equations (1) to (2), the differential equations can be written as:

$$\frac{dn_0}{dt} = aG(d_p + d_b)^3 \frac{\phi}{\pi d_b^3/6} \alpha_0 n_0 \quad (6)$$

$$\frac{dn_{i\max}}{dt} = aG(d_p+d_b)^3 \times \frac{\phi}{\pi d_b^3/6}\left(a_i\left(1-(i_{\text{msx}}-1)\frac{d_b^2}{d_p^2}\right)n_{i-1} - \left(1-i\frac{d_b^2}{d_p^2}\right)n_i\right), \quad (7)$$

$i = 1$ to $1_{\max} - 1$

$$\frac{dn_{i\max}}{dt} = aG(d_p+d_b)^3 \frac{\phi}{\pi d_b^3/6} a_i\left(1-(i_{\text{msx}}-1)\frac{d_b^2}{d_p^2}\right)n_{i_{\max}} - 1 \quad (8)$$

Equations (6) to (8) are subject to the initial conditions $n_0 = N_0$ and $n_i = 0$ for all $i \geq 1$, when $t = 0$ in order to determine the values of n_i after a retention time of $t = t_{\text{contact}}$ in the contact zone. Introducing the dimensionless variables $t^* = t/t_{\text{contact}}$ and $n^* = n_i/N_0$, Equations (6) to (8) can be represented for dimensionless form as:

$$\frac{dn_0^*}{dt^*} = -\kappa n_0^* \quad (9)$$

$$\frac{dn_i^*}{dt^*} = \kappa\left(\left(1-(i-1)\frac{d_b^2}{d_p^2}\right)n_{i-1}^* - \left(1-i\frac{d_b^2}{d_p^2}\right)n_i^*\right), \quad (10)$$

$i = 1$ to $i_{\max} - 1$

$$\frac{dn_{i\max}^*}{dt^*} = \kappa\left(1-(i_{\max}-1)\frac{d_b^2}{d_p^2}\right)n_{i_{\max}-1}^* \quad (11)$$

Dimensionless flotation rate constant κ, can be represented as:

$$\kappa = \frac{6aGt_{\text{contact}}\left(1+\frac{d_p}{d_b}\right)^3 \phi\alpha_0}{\pi} \quad (12)$$

Applying Laplace transformation, the number of flocs attached with bubbles can be represented as:

$$n_i^* = \binom{d_p^2/d_b^2}{i}\exp(-\kappa t^*)\left(\exp\left(\frac{\kappa t^*}{d_p^2/d_b^2}\right) - 1\right) \quad (13)$$

$i = 0$ to $i_{\max} - 1$

$$n_{i_{\max}}^* = 1 - \sum_{i=0}^{i_{\max}-1} n_i^* \quad (14)$$

where the generalized combinational is defined as Equation (15):

$$\binom{x}{i} = \frac{x!}{i!(x-i)!} = \frac{x(x-1)\cdots(x-(i-1))}{i(i-1)\cdots(2)(1)} \tag{15}$$

The diameter of bubble-floc agglomerate (d_{pb}) and the density of bubble-floc agglomerate (ρ_{pb}) composing one particle (or floc) and i-bubbles are calculated using Equations (16) and (17).

$$d_{pb} = (d_p^3 + i d_b^3)^{1/3} \tag{16}$$

$$\rho_{pb} = \frac{\rho_p d_p^3 + i \rho_b d_b^3}{d_p^3 + i d_b^3} \tag{17}$$

The rise velocity of the agglomerate is determined by solving a series of physical equations using the least squares method known as the Levenberg-Marquardt algorithm as an initial trial value with Stokes approximation represented by Equation (18) (Clift *et al.* 1978; Leppinen *et al.* 2001).

$$v_{i,cr} = \frac{(\rho_w - \rho_{pb}) g d_{pb}^2}{18\mu} \tag{18}$$

The maximum number of attached bubbles on a floc suggested by Matsui *et al.* (1998) can be written as:

$$i_{max} = \lfloor \max(1, c(d_p/d_b)^2) \rfloor \tag{19}$$

where $[x]$ is the largest integer and c is a numeric constant. In this study, we used the empirical value $c = 1$ as suggested by Matsui *et al.* (1998).

MATERIALS AND METHODS

DAF jar tester for observation of bubble-floc agglomerates

A jar tester equipped with bubble-supplying apparatus and particle image analyser (PIA) was used to measure the size of a bubble and a floc and sedimentation as well as flotation velocity as shown in Figure 1. We were able to determine the rise velocity by tracking a series of images taken from continuous photographs of bubbles or bubble-floc agglomerates. The PIA was composed of a microscope, a high speed CCD camera, and an image analyser (Image-Pro Plus v. 5.0). The flow cell was vertically placed on the upper part of the jar tester of PIA, so that it could take the photographs of static and moving images through a microscope and a high-speed camera after fixing underwater particles in the flow cell. With photographed images, the image analyser analyses the velocity vector and the size of particles using the tracking technique.

In addition, all of the capturing and tracking of images to measure the rise velocity of bubble-floc agglomerates was performed within about 10 cm height difference of the flotation column. The measurement was influenced by neither the water surface condition nor open system conditions such as air because the images were taken completely within a short time before reaching the water surface. The possible size change of attached bubbles on a floc caused by the difference of water pressure in the course of the tracking was considered so little that it was ignored in the course of prediction and calculation of the rise velocity of bubble-floc agglomerates.

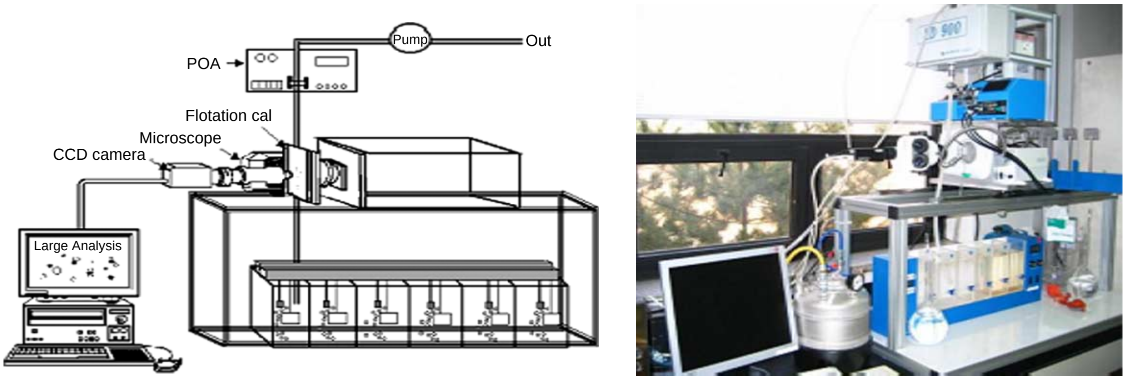

Figure 1 | Schematic diagram and photograph of the jar tester equipped with bubble-supplying apparatus and PIA.

Table 1 | Features of the raw water quality used in this experiment

Turbidity (NTU)	1.4 ± 0.3
Alkalinity ($mg\,l^{-1}$ as $CaCO_3$)	27.5
Temperature (°C)	20 ± 2
pH	7.17

Coagulation in the jar tester was carried out with a mixing intensity of $1,100\,s^{-1}$ for 5 seconds followed by flocculation with a mixing intensity of $50–70\,s^{-1}$ for 10 minutes. Most of the measurements and the evaluations were performed under the same operation conditions in order to minimize the observation errors. For the flotation conditions of this experiment, the pressure of the saturator was $5\,kg\,cm^{-2}$ and a recycle ratio of 15% was applied. Three minutes elapsed after dosing of bubbles to make the agglomerates in the jar, the rise velocity of bubble-floc agglomerates taken through the sampling port of the middle base of the jar was measured along the vertical flotation tube. The raw water used in this experiment was taken from the S water treatment plant; this water is typical of the range of raw water quality for drinking water treatment works, as shown in Table 1. PAC (11% as Al_2O_3, poly aluminum chloride) was used as coagulant, and other experimental conditions were within the typical range of the DAF process (Kwak *et al.* 2005).

Prediction of attached bubble number and rise velocity

By using the equations described above, the maximum rise velocity of the bubble-floc agglomerate can be predicted as a function of the bubble and floc sizes. The maximum rise velocity of bubble-floc agglomerates is determined on the basis of the possible maximum number of bubbles attached on one floc. The number of attached bubbles in terms of mixing time in a contact zone can be obtained by Equations (1) to (14) applied with population balance. Table 2 presents the parameters of extended equations including population balance to predict the rise velocity of the agglomerate and the number of bubbles on a floc. On the basis of the simulated results for the maximum attached bubble number, the maximum rise velocity in terms of floc diameters was calculated by Equations (16) to (19).

RESULTS AND DISCUSSION

The maximum number of attached bubbles on a floc

The maximum number of attached bubbles on a floc represents the largest number of bubbles which can attach ideally on the surface of a single floc in the contact zone of the DAF process. Figure 2 shows the simulated results using population balance to predict the number of attached bubbles on a floc in terms of dimensionless time for the operational conditions applied with different air bubble numbers and floc sizes. There was negligible

Table 2 | Parameters using the population balance model in the DAF process

Parameters	Value	Unit	Reference
Diameter of bubble (d_b)	$2.0–12.0 \times 10^{-5}$	m	
Diameter of floc or particle (d_p)	$1.0–80.0 \times 10^{-5}$	m	Kwak *et al.* (2005)
Density of water (ρ_w) at 293.15 K	1.0×10^3	$kg\,m^{-3}$	
Density of bubble (ρ_b) at 293.15 K	1.17×10^{-3}	$kg\,m^{-3}$	Liers *et al.* (1996)
Viscosity of water (μ) at 293.15 K	1.306×10^{-2}	kg/m·s	Reid *et al.* (1987)
Temperature of water (T)	293.15	K	
Numerical constant (a)	5.0×10^4	–	
Turbulent dissipation of energy (ε_0)	6.0×10^{-3}	$W\,m^{-3}$	
Bubble volume concentration (ϕ)	0.0046	$m^3\,m^{-3}$	Edzwald (1995)
Initial adhesion efficiency (α_0)	0.3	–	Fukushi *et al.* (1995)
Surface loading rate (v_{SL})	1.8–27.0	$m\,s^{-1}$	

difference between a bubble number concentration of 10,000 and 50,000 as shown in Figure 2 (a) and (b). However, in the case of the floc diameter enlarged from 200 to 300 μm, there was a notable difference as shown comparatively in Figure 2 (b) and (c). The difference in the maximum attached bubble number as well as the attached velocity may be attributed to the increasing surface area of the floc. The floc size affected the number of attached bubbles on a floc much more than the bubble concentration when it is supplied with a sufficient number of bubbles to attach on the surface of floc. According to the simulated results using the equations described above on the basis of population balance, the maximum number of bubbles attached on a floc was 11 for the floc diameter of 200 μm and 25 for the floc diameter of 300 μm. Besides, the time required for bubbles to adhere to the larger floc (diameter 300 μm) was three times faster than that for the floc diameter of 200 μm.

If the rise velocity of the agglomerate alone is considered and if the collision efficiency is ignored, we suggest that the larger floc would be more effective for rapid separation of the bubble-floc agglomerates.

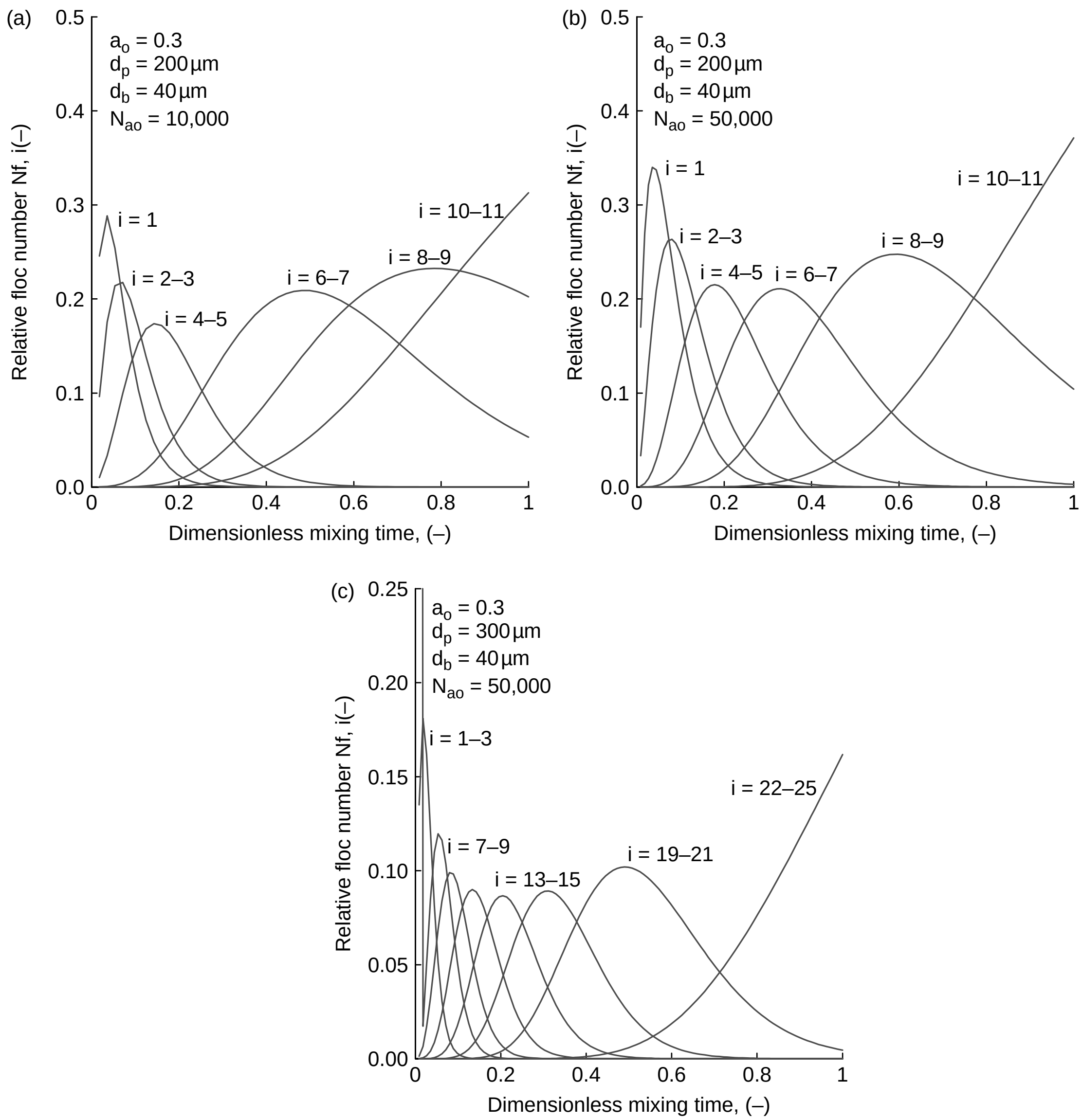

Figure 2 | Number of attached bubbles on a floc simulated in terms of mixing (contact) time.

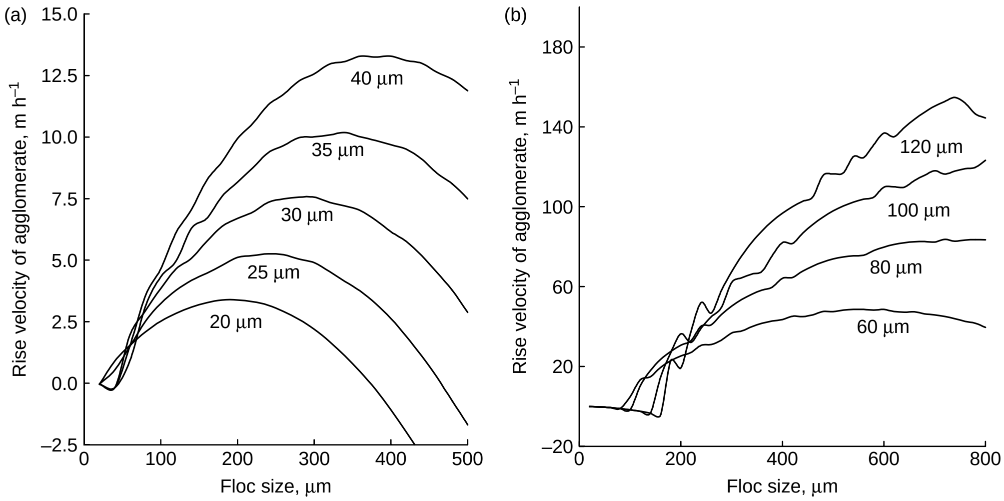

Figure 3 | Maximum rise velocity of bubble/floc agglomerates as a function of bubble diameter.

Maximum rise velocity of the bubble-floc agglomerate

Considering the range of applied bubble size in the DAF process in general, bubbles can be classified roughly into two groups (smaller group: db = 20–40 μm; larger group: db = 60–120 μm). As shown in Figure 3, the rise velocity (over zero) represents the upward flotation of agglomerate, while negative values of rise velocity denote the downward sedimentation of agglomerate subjected to the absence of flux. For the smaller group of bubble size shown in Figure 3(a), the rise velocity of the agglomerate is as low as below $15\,\mathrm{m\,h^{-1}}$ compared with the larger bubble group. As the bubble size increased, the maximum rise velocity of the agglomerate was increased sharply. In addition, the highest value of the maximum rise velocity moved to the larger floc size as the bubble size increased. Contrary to the fact that the larger bubble is more effective on the basis of this result, the larger bubble has been found to bring about a low collision efficiency between bubble and flocs (Edzwald 1995; Han *et al.* 2001). Moreover, controlling the bubble size is actually hard to perform in the field.

Recently, the hydraulic loading rate directly affecting the flotation efficiency increased to about $40\,\mathrm{m\,h^{-1}}$ (Haarhoff & Edzwald 2004). To design the high rate flotation processes, the number of attached bubbles and the rise velocity of agglomerate depending on bubble sizes should be taken into account carefully.

Observation of initial bubble diameter and rise velocity of bubble-floc agglomerate

The size of the flocculated flocs using PIA was directly measured using a captured image, and the images of flocs

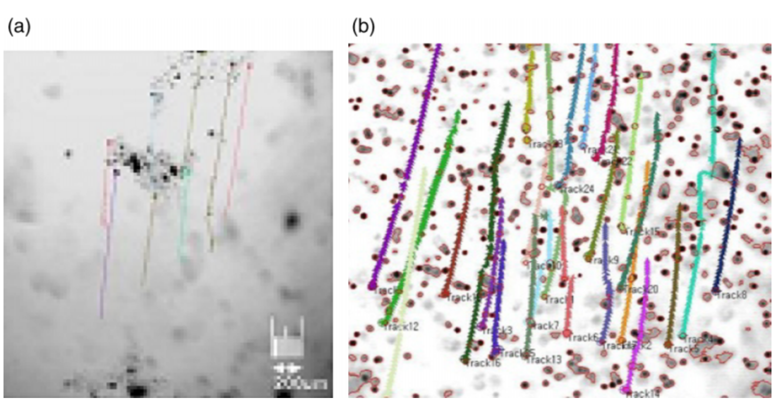

Figure 4 | Photograph of rise velocity tracking: (a) captured image from CCD camera; (b) tracking image of bubble-floc agglomerates.

were analysed for the calculation of the rise velocity using a tracking technique (Figure 4). The results of the observation by PIA and the tracking method in the jar tester are shown in Table 3. A series of images of the rising bubble-floc agglomerates taken by the random sampling method in the flotation column were captured at regular, short time intervals. The initial bubble diameter measured before the experiment without flocs was about 40 μm on average, and the distribution range was mostly from 30 μm to 50 μm similar to previous work (Kwon *et al.* 2005).

Verification of difference between prediction and observation

There was no similarity between the observed rise velocity measured by PIA and the predicted value, contrary to what we had expected, as shown in Figure 5. If the results of prediction were free from fault, the difference could be possibly attributed to two kinds of causes: the bubble size was enlarged during the experiment, and the actual number of attached bubbles on a floc was greater than the predicted values.

We tried to find out the cause of the difference in the course of measurement from the sampling port in the jar to the observation point in the flow tube. To verify the enlargement of bubble size in the course of the contact and separation processes, we chose the direct measurement of bubble size distribution using PIA. However, due to shadows and blocking of the agglomerate by the floc, it was very difficult to accurately estimate the bubble size in agglomerates after adhesion between bubble and floc without any observational errors. Furthermore, counting the number of attached bubbles on a floc was nearly

Table 3 | Measured results for the flocs, bubbles and bubble-floc agglomerates in the experiment

Description	Physical characteristics of agglomerate samples A	B	C	D	E
Diameter of floc in agglomerate, d_p (μm)	285	390	440	535	695
Rise velocity of agglomerate, v_{pb} (m h^{-1})	33.5	21.4	53.0	43.7	54.4

Note: Density of flocs in agglomerate, ρ_p (kg m^{-3}) = 1,000.8–1,011.1 (Kwon *et al.* 2005).

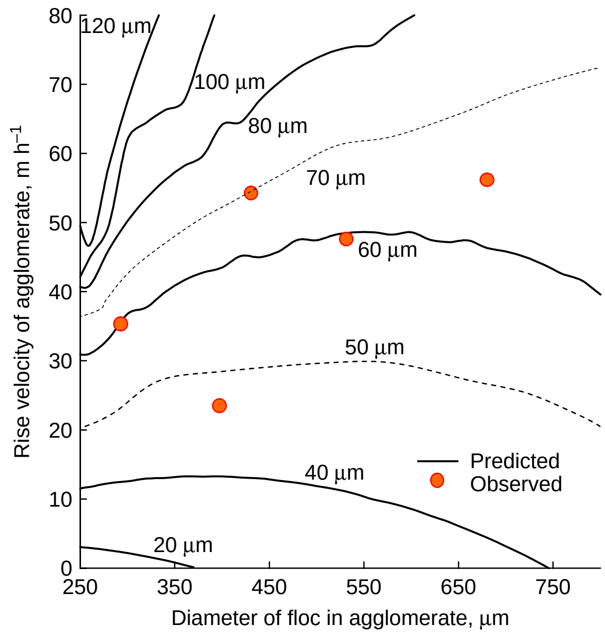

Figure 5 | Comparison between predicted and observed values for rise velocity of agglomerates.

impossible because of the vulnerable coherence force between bubbles and flocs. In the course of sampling and handling, the bubble-floc agglomerate bubbles were too easily detached from the surface of the floc.

Otherwise, to verify the difference between observed and predicted values, the number of attached bubbles on a floc, *i*, was calculated as described above by Equations (16) to (19) using the observed rise velocity values. The maximum number of bubbles attached on a floc calculated from the measured values of the rise velocity of the bubble-floc agglomerate was greater than we had expected as shown in Table 4 and Figure 6. In the case of a bubble diameter of 40 μm, there were hundreds of bubbles attached on the surface of one floc while there were no changes in the bubble size. This large number of bubbles, however, was impossible to attach on the surface of such a small floc in practice. On the basis of many previous studies, the calculated values of the number of attached bubbles on a floc were not acceptable practically. There might be other reasons leading to the excessive predicted values based on the rise velocity of the bubble-floc agglomerate observed by the tracking method. The enlargement of bubble size could be considered as the cause since the predicted value resulted in too many attached bubbles on a floc.

 Journal of Water Supply: Research and Technology—AQUA | 58.2 | 2009

Table 4 | Calculation results for the number of attached bubbles on a floc based on the bubble size

	Number of attached bubbles on a floc			
Diameter of floc, d_p (μm)	Bubble diameter 40 μm	Bubble diameter 60 μm	Bubble diameter 80 μm	Bubble diameter 100 μm
285	101	30	13	7
390	77	23	10	3
440	228	68	29	15
535	218	65	27	14
695	344	102	43	22

Possible cause of the difference between predicted and observed values

Since the maximum number of attached bubbles on a floc calculated from the measured values of the rise velocity of the bubble-floc agglomerate was an impractical value as discussed above, it led us to consider that there were a number of possible mechanisms which could conceivably explain the observations. It was considered that three possible causes could give rise to the differences between predicted and observed values as follows.

First of all, the bubble-floc interaction does not stop when the suspension leaves the contact zone, but continues throughout the white-water region in the separation zone.

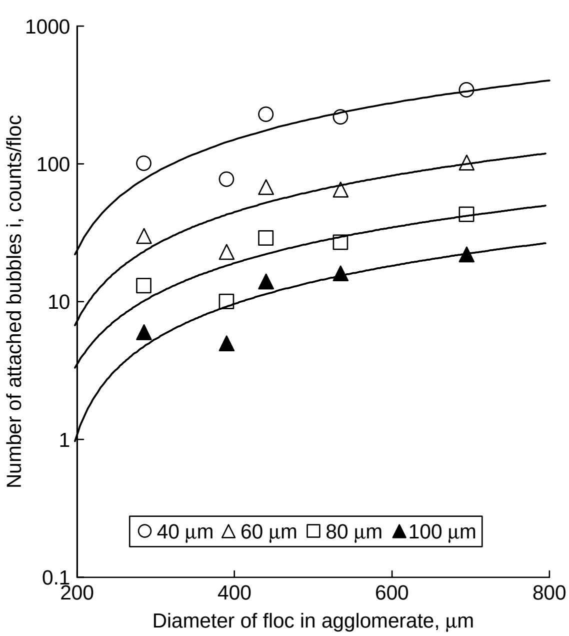

Figure 6 | Calculated number of attached bubbles on a floc as a function of bubble diameter.

The modelled number of bubbles per floc at dimensionless time 1 as we have assumed could thus be an underestimate. Second, there could be a slight change of bubble size from the decrease of physical pressure depending on the water depth or the variation of surface tension for bubble-floc agglomerates that may be caused in the course of the observation. There could be some decompression of the bubbles as they rise from the bottom of the tank to the top. Although the bubble sizes enlarged by decompression could contribute a small part of the differences between predicted and observed values, the enlargement of bubble size could possibly be much larger in the field since there is a considerable pressure change from the bottom to the surface in a deep flotation tank. Furthermore, there also could be a decrease in surface tension as the bubbles come into contact with the flocs to allow the bubbles to further decompress. Third, as the bubbles attach to the flocs and come very close together, they may touch and coalesce on the surface of the flocs, thus freeing up some space for new bubbles to attach. Therefore, it was considered that the empirical value c of Equation (19) could be greater than 1 for the maximum number of attached bubbles on a floc. On the other hand, the bubbles could coalesce even before they contact the flocs and therefore grow. In this study, however, because the observation was carried out in the narrow column of the PIA by the tracking method, the possibility of coalescence was comparatively unlikely.

CONCLUSIONS

The rise velocity of bubble-floc agglomerates was investigated to verify the comparison between theoretical and observed results. However, there was no similarity between the observed rise velocity measured by PIA and the predicted values, contrary to what we had expected. Furthermore, the simulated results using population balance to predict the maximum number of attached bubbles on a floc were too impractical to accept under the actual condition of the surface of the floc if there was no change of bubble size. These findings led us to suggest that there were three possible causes which could conceivably explain the observations. Regarding the prediction using population balance, the predicted number of bubbles on a floc at dimensionless time 1 as we have assumed could be an underestimate, or the empirical value *c* for the maximum number of attached bubbles on a floc could be greater than 1. In addition, there could be a slight change of bubble size from the decrease of physical pressure depending on the water depth or the variation of surface tension for bubble-floc agglomerates that may be caused in the course of the observation. It was suggested that the differences between predicted and observed values could be attributed to one or more of these mechanisms.

ACKNOWLEDGEMENTS

This work was supported by Grant No. R01-2004-000-11029-0 from the Korea Science & Engineering Foundation.

REFERENCES

Clift, R., Grace, J. R. & Weber, M. E. 1978 *Bubbles, Drops, and Particles*. Academic Press, New York.

Edzwald, J. K. 1995 Principles and applications of dissolved air flotation. *Water Sci. Technol.* **31**(3–4), 1.

Fukushi, K., Tambo, N. & Matsui, Y. 1995 A kinetic model for dissolved air flotation in water and wastewater treatment. *Water Sci. Technol.* **31**(3–4), 37–47.

Haarhoff, J. & Edzwald, J. K. 2004 Dissolved air flotation modelling: insights and shortcomings. *J. Water Supply Res. Technol.–AQUA* **53**(3), 127–150.

Han, M. Y., Kim, W. T. & Dockko, S. 2001 Collection efficiency factor of bubble and particle (α_{bp}) in DAF: theory and experimental verification. *Water Sci. Technol.* **43**(8), 139–144.

Jung, H. J., Lee, J. W., Choi, D. Y., Kim, S. J. & Kwak, D. H. 2006 Flotation efficiency of activated sludge flocs using population balance model in dissolved air flotation. *Korean Chem. Eng. Res.* **23**(2), 271–278.

Kwak, D. H., Kim, S. J., Lee, H. K., Jung, H. J., Lee, J. W. & Chung, P. G. 2002 Hydrodynamic collision efficiency and flotation characteristics of inorganic particles in DAF process. *J. Korean Soc. Water Wastewater* **16**(6), 655–662.

Kwak, D. H., Jung, H. J., Kim, S. J. & Lee, J. W. 2005 Separation characteristics of inorganic particles from rainfalls in dissolved air flotation: a Korean perspective. *Sep. Sci. Technol.* **40**, 3001–3016.

Kwon, S. B., Min, J. H., Lee, S. J., Ahn, H. W. & Wang, C. K. 2005 Evaluation of floc formation conditions for increasing flotation velocity in DAF process. *IWA Particle Separation 2005*, Seoul, Korea, 1–3 June 2005.

Leppinen, D. M., Dalziel, S. B. & Linden, P. F. 2001 Modeling the global efficiency of dissolved air flotation. *Water Sci. Technol.* **43**(8), 159.

Liers, S., Baeyens, J. & Mochtar, I. 1996 Modeling dissolved air flotation. *Water Environ. Res.* **68**(6), 1061.

Malley, J. P. & Edzwald, J. K. 1991 Conceptual model for dissolved-air flotation in drinking water treatment. *J. Water Supply Res. Technol.–AQUA* **40**(1), 7–17.

Matsui, Y., Fukushi, K. & Tambo, N. 1998 Modeling, simulation and operation parameters of dissolved air flotation. *J. Water Supply Res. Technol.–AQUA* **47**, 9.

Reid, R. C., Prausnitz, J. M. & Poling, B. E. 1987 *The Properties of Gases and Liquids*, 4th edition. McGraw-Hill, New York.

Rodrigues, R. T. & Rubio, J. 2003 New basis for measuring the size distribution of bubbles. *Miner. Eng.* **16**, 757–765.

Schers, G. J. & Van Dijk, J. C. 1992 Chemical water and treatment II. In: *Dissolved-Air Flotation: Theory and Practice, 5th Gothenburg Symposium*, France, pp. 223–246.

Suffman, P. G. & Turner, J. S. 1956 On the collision of drops in turbulent clouds. *J. Fluid Mech.* **1**, 16–30.

Tambo, N. & Fukushi, K. 1985 A kinetic study of dissolved air flotation. *J. Jpn. Water Works Assoc.* **606**, 22–30.

Tambo, N., Hozumi, H. & Watanabe, Y. 1981 A rational design of flocculator-I. *J. Jpn. Water Works Assoc.* **50**(6), 20–27.

Tambo, N., Fukushi, K. & Matsui, Y. 1985 An analysis of air bubble attachment process of dissolved air flotation. *J. Jpn. Water Works Assoc.* **610**, 2–11.

First received 10 March 2008; accepted in revised form 21 August 2008. Available online January 2009